Desalination and Water Treatment
www.deswater.com
doi: 10.1080/19443994.2014.913208

55 (2015) 199–209
June

Taylor & Francis
Taylor & Francis Group

Removal of Cu(II) and Ni(II) by ion exchange resin in packed rotating cylinder

N.K. Amin[a], O. Abdelwahab[b,*], E.-S.Z. El-Ashtoukhy[a]

[a]*Faculty of Engineering, Chemical Engineering Department, Alexandria University, Alexandria, Egypt*
[b]*Environmental Division, National Institute of Oceanography and fisheries, Kayet Bay, El-Anfushy, Alexandria, Egypt, Tel. +201221093161; Fax: +2033877470; email: olaabdelwahab53@hotmail.com*

Received 7 November 2013; Accepted 3 April 2014

ABSTRACT

The removal of copper and nickel ions from aqueous solutions was evaluated using an ion-exchange resin, purolite C100-MB packed in a perforated rotating basket reactor. The cation-exchange performance of the resin was determined by batch equilibrium method. The present reactor can replace batch agitated vessel where the resin was fluidized by rotating impeller. The effect of rotational basket speed, pH, contact time, temperature, and coexisting metal ions were demonstrated. The reusability of the resin was also studied to estimate the effectiveness of the purolite C100-MB resin. Equilibrium experimental data were successfully described by Langmuir isotherm models. An empirical design procedure based on sorption equilibrium conditions was used for predicting the size of ion exchange reactor. Experimental data were analyzed according to the surface reaction and intraparticle models. Kinetic experiments demonstrated that experimental data for purolite C100-MB resin obey pseudo-second-order models with rates limited by particle diffusion. Various thermodynamic parameters have been calculated. The sorption process of copper and nickel ions onto purolite C100-MB resin was found to be spontaneous and exothermic process.

Keywords: Ion exchange; Design; Copper; Nickel; Kinetics; Basket reactor

1. Introduction

Large amounts of toxic and carcinogenic metals have been released into the environment, especially in industrial areas as waste streams from mining operations, metal-plating facilities, power generation facilities, electronic device manufacturing units, and tanneries [1–3]. These species even at very low concentrations can produce toxic effects in humans that can inhibit cellular activities and result in the development of serious diseases and physiological problems such as a variety of cancers [4]. According to WHO guidelines, the Cu(II) ions are considered toxic with permissible level in drinking water of 1.3–2 mg/L. The maximum admissible concentration of Ni(II) in aqueous solution is only 0.02 mg/L [5].

Due to the mounting demand for industries producing heavy metals, there is a possibility of higher level of Cu(II) and Ni(II) in the effluents or the water bodies which are in close proximity to such industries. Therefore, the removal of Cu(II) and Ni(II) from wastewaters, in order to reduce their concentration below the acceptable range, is highly warranted. At this juncture, the applicability of various methods

*Corresponding author.

developed so far for the removal of Cu(II) and Ni(II) from effluents should be critically reviewed and more suitable methods need to be proposed. Several processes are available for the removal of heavy metals from water and wastewater including chemical precipitation, adsorption, ion exchange, flotation, membrane filtration, electrochemical treatment, and coagulation–flocculation. The advantages and disadvantages of each process were summarized by O'Connell et al. [6,7]. Adsorption and ion exchange processes can be used for the removal of heavy metals from wastewater. Moreover, more attention has been paid on the ion-exchange process with polymeric resins, which shows an effective, straightforward, and recyclable purification in comparison with other methods [8]. A wide variety of heavy metals can be removed from the liquid phase at significant quantities and kinetics and are usually fast. The drawbacks are that the performance depends on sorbent's selectivity towards the metal, while in many cases pre-treatment is required to improve its adsorption capacity [9].

A new reactor design was used to study the removal of Cu(II) and Ni(II) by cation exchange resin. The fundamental adsorption behaviors of copper and nickel onto purolite C100-MB resin including pH effects, adsorption equilibrium, kinetics, and thermodynamics were investigated. Moreover, the reuse of the used resin was also performed, since the reuse and recycling of the used adsorbents is of great importance in practical applications. In addition, the rate-determining step of the removal of Cu(II) and Ni(II) was determined based on the experimental results obtained. The adsorption selectivity was also analyzed for simulation solutions containing binary mixtures. The new rotating basket reactor design has an advantage via ordinary batch reactor in ease of separating the resin from the solution without the need of filtration.

2. Experimental section

2.1. Materials and reagents

The ion exchange resin used in experiments was the gel-type strong acid purolite C100-MB resin with sulfonic acid $–SO_3H$ group. It was supplied by the water treatment plant of SIDPEC, Alexandria, Egypt. Physical properties and specifications of the resin as reported by the supplier are shown in Table 1.

Analytical-grade copper sulfate ($CuSO_4.5H_2O$), nickel chloride ($NiCl_2.6H_2O$), NaOH, and HCl were provided by Sigma–Aldrich, Germany. Stock solutions of copper and nickel metal ions were prepared using distilled water.

Table 1
Typical physical and chemical characteristics of purolite C100MBH

Property	Purolite C-100MBH
Type	Strong acid cation
Physical form	Small, unsoluble beads
Functional group	Sulfonic acid
Total capacity (eq dm^{-3} of resin)	1.8
Moisture retention (%)	50–56
Mean size typical (mm)	0.6–0.9
Uniformity coefficient (max)	1.7
Reversible swelling (max) (%)	8
Specific gravity (g cm^{-3})	1.2
Temperature limit (°C)	120
pH limits	0–14
Measured porosity (%)	37.5
Price/bag ($)	105–168

2.2. Ion exchange pretreatment

The resin was supplied in the hydrogen form. However; the hydrogen content of the resin may not be consistent. Therefore, pretreatment of the resin was required to ensure consistency of the experimental results and control the hydrogen content. The resin was immersed in 1 M NaOH solution for 45 min to replace all hydrogen ions by sodium ions, then it was immersed in 1 M HCl for 45 min to replace all sodium ions by hydrogen ions. The resin was then washed with distilled water to remove excess Cl^- groups. After that, it was dried several days in an ambient temperature then in the oven at 90°C and allowed to cool. Finally, it was sieved and packed to be used in experiments.

2.3. Ion exchange experiments

2.3.1. Apparatus

The experimental setup used in the present study consists of plexi-glass cylindrical container fitted with four rectangular baffles fixed to the container wall 90° from one another. The resin particles were packed in a perforated basket. It was fitted at the center to an isolated stainless steel shaft which was connected to a variable speed motor (Fig. 1). The motor rotational speed was varied within the range 50–300 rpm. Three liters of metal solution were used in each experiment. A typical experimental runs lasted 60 min, where samples of 5 mL were taken from reaction solution each time interval and analyzed for metal ion concentration by atomic absorption spectrophotometer using Varian Spectra AA 55B. Temperature of solution was

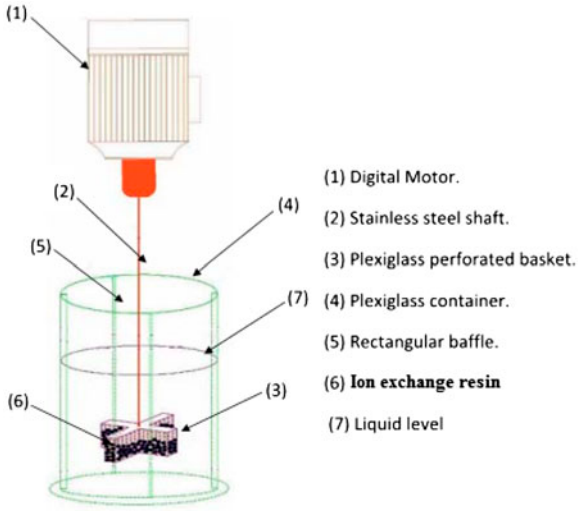

Fig. 1. Experimental setup.

controlled using a thermo-stated water bath and ranged from 20 to 50 °C.

2.3.2. Adsorption of Cu(II) and Ni(II) at different initial solution pH

The influences of different initial solution pH to the adsorption of copper and nickel by purolite C100-MB were investigated. The pH ranged from 2 to 8, and speed of rotation from 50 to 200 rpm at constant initial concentration 500 mg $dm^{-3}$of copper or nickel ions. Resin was added to the solution in the solid to liquid ratio, S/L, of 6 g dm^{-3}. The pH of Cu(II) and Ni (II) solutions was adjusted using either 0.1 M HCl or 0.1 M NaOH. The resin was added to the metal solutions with different initial pH under continuous stirring at room temperature for an hour. The metal ion concentrations were analyzed and adsorption capacities of heavy metal ions were calculated.

2.3.3. Adsorption equilibrium experiments

The adsorption equilibrium experiments of purolite C100-MB were carried out at 20 °C and pH 5.5. The initial metal concentration was ranged from 400 to 800 mg dm^{-3} for copper and from 400 to 700 mg dm^{-3} for nickel. The resin was weighed and immerged in metal solutions with various initial concentrations under continuous stirring for 3 h. The initial and final metal concentrations were measured. The adsorption of metal ions at equilibrium, q_e (mg g^{-1}), were calculated from the following equation:

$$q_e = \frac{(C_0 - C_e)V}{M} \quad (1)$$

where C_0 and C_e (mg dm^{-3}) are the initial and final metal concentrations, V (dm^3) is the volume of the metal solution, and M (g) is the weight of the resin.

2.3.4. Kinetics adsorption experiments

The kinetic experiments of ion exchange were conducted at 20 °C and pH 5.5. The initial concentrations were ranged from 400 to 800 mg dm^{-3} for copper and from 400 to 700 mg dm^{-3} for nickel. S/L ratio was 6 g dm^{-3}. The resin was loaded in metal solutions under continuous stirring at 200 rpm. At desired time intervals, sample solution was taken out and analyzed for metal concentration. Meanwhile, the adsorption of metal ions at any time t, q_t (mg g^{-1}), was calculated from the following equation,

$$q_t = \frac{(C_0 - C_t)V}{M} \quad (2)$$

where C_t (mg dm^{-3}) is the concentrations at time t (min).

2.3.5. Adsorption selectivity

The competitive adsorption performances for binary metal systems were carried out at pH 5.5, 20 °C, and S/L ratio = 6 g dm^{-3} at 150 rpm. The concentration of the solution was 400 mg dm^{-3} while the studied copper to nickel ratios were 1:1, 1:2, 1:4, 2:1, 4:1. Selectivity between Cu(II) and Ni(II) can be quantified in terms of the distribution coefficient in binary system (K_D) which could be expressed by the formula given below [10]:

$$K_D = \frac{\text{uptake of heavy metal by resin per unit of dry resin}}{\text{remaining concentration of heavy metal in solution}} \quad (3)$$

2.3.6. Desorption studies

The recovery and reusability of the adsorbent material is an important parameter related to the application potential of adsorption processes. In this study, purolite C100-MB resin was subjected to 0.1 M HCl solution in order to determine desorption properties of the resin. The bound copper(II) and nickel species resin were immersed in 1 M HCl for

45 min, then washed with distilled water to remove the excess of Cl^- groups.

The adsorption–desorption experiments were conducted totally for four cycles using the same concentration of Cu(II) or Ni(II) species in solutions containing the same resin.

3. Results and discussion

3.1. Effect of pH and speed of rotation on metal removal

The pH of solution affects surface charge of ion exchange and degree of ionization and speciation of heavy metal. Normally metal adsorption is fully dependent on pH condition of water as mentioned in previous studies [11]. In order to investigate the effect of pH on removal of copper and nickel ions, experiments were performed in the pH range from 2.0 to 8. Effect of pH on adsorption capacity shows that the optimal uptake of Cu(II) and Ni(II) occurred at pH 5.5 as shown in Fig. 2((a) and (b)). However, at lower pH values, the capacity of adsorption was decreased. This is due to the fact that H^+ ion was considered as a competitive ion in the adsorption process and the solution pH influences the ionization of surface functional groups. Therefore, very low adsorption of the metal takes place from high acidic solutions [12]. While, at high pH values, decrease in adsorption capacity which achieved by resin can be described with formation of $Cu(OH)_2$ and $Ni(OH)_2$ during reaction of Cu(II) and Ni(II) ions with OH^-_2. In this state, hydrolysis accompanied by precipitation of metal hydroxides may occur. These results are in good agreement with those described by previous work [12–14]. Fig. 2((a) and (b)) clearly shows that the amount of Cu(II) and Ni(II) adsorption increases with the increase in agitation speed up to 200 rpm. As the agitation speed increases, there develops a proper interaction between heavy metal in solution and the adsorption sites on the purolite C100-MB. This may enhance effective transfer of metal ions species onto the resin surface [5].

3.2. Ion-exchange equilibrium

Ion-exchange equilibrium of Cu(II) and Ni(II) were measured at 20 °C and pH 5.5. Experimental data were analyzed by the Langmuir, Freundlich, Tempkin, and Dubinin Radushkevich isotherms [15,16]:

Langmuir equation:

$$q_e = \frac{Q_m K_L C_e}{1 + K_L C_e} \tag{4}$$

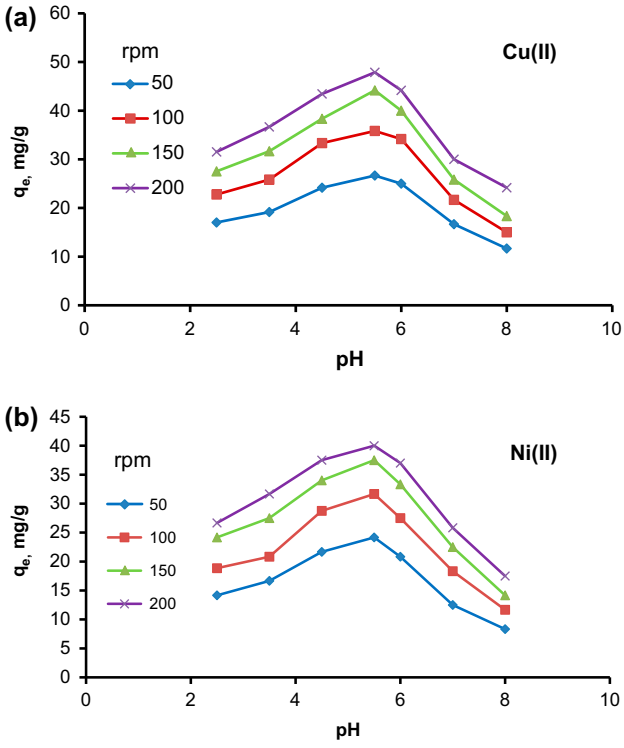

Fig. 2. Effect of pH on adsorption capacity at different speed of rotation for (a) Copper ions, (b) Nickel ion; (initial metal concentration = 500 mg dm^{-3}, time = 1 h, S/L = 6 g dm^{-3}).

Freundlich equation:

$$q_e = K_F C_e^{n_F} \tag{5}$$

Tempkin equation:

$$q_e = B \ln (K_T C_e) \tag{6}$$

where

$$B = \frac{RT}{b_T} \tag{7}$$

Dubinin–Radushkevich (D–R) equation:

$$q_e = q_S \exp(-K_{DR}\varepsilon^2) \tag{8}$$

where

$$\varepsilon = RT \ln\left(1 + \frac{1}{C_e}\right) \tag{9}$$

where q_e is the metal concentration in the resin phase at equilibrium and C_e is the metal concentration in the solution phase at equilibrium; Q_m, K_L, K_F, n_F, b_T, K_T, q_s, K_{DR}, and ε represent the Langmuir, Freundlich, Tempkin, and R-D isotherm constants respectively. The mean free energy E of sorption per molecule of the sorbate can be computed from relationship: ($E = 1/(2\ K_{DR})^{0.5}$). All of these equations can be rearranged to a linear relationship, from which the coefficients can be determined by the slopes and intercepts. The adsorption isotherm coefficients obtained for the ion exchange of Cu(II) and Ni(II) onto purolite C100-MB resin are listed in Table 2. The data were further analyzed using the Chi-square test to confirm the best fit isotherm for the ion exchange of copper and nickel ions using purolite C100-MB resin. The test was expressed as follows [16]

$$X^2 = \sum (q_{e,\exp} - q_{e,\mathrm{calc}})^2 / q_{e,\exp} \quad (10)$$

where $q_{e,\exp}$ is the experimental data of the mass of adsorbed heavy metal per unit resin (mg g^{-1}), $q_{e,\mathrm{calc}}$ is the equilibrium mass of adsorbed heavy metal per unit resin obtained by calculating from the model (mg g^{-1}). The values of X^2 for all isotherms are presented in Table 2.

The experimental adsorption data were fitted based on the aforementioned isotherm models. Based on R^2 and X^2 in Table 2, the Langmuir adsorption isotherm provides a better fit to the experimental data of copper and nickel than the Freundlich, Tempkin, and R-D approach. Meanwhile, the coefficients for Freundlich and Temkin models also provide good fitting to the data, whereas those for D-R model were much lower. According to Langmuir model, the calculated maximal Cu(II) and Ni(II) uptakes of purolite C100-MB were quite close to their corresponding experimental data. From Fig. 3(a)–(b), it was found that the Langmuir isotherm simulated curves fitted the experimental data in a fairly good way. They all revealed that Langmuir model proposed the most satisfactory description on the Cu(II) and Ni(II) adsorp-

Table 2
Isotherm constants for Cu(II) and Ni(II) sorption on ion exchange resin purolite C100-MB

		Langmuir isotherm constants				Freundlich isotherm constants			
Metal	rpm	Q_m	K_L	R^2	X^2	K_F	n	R^2	X^2
Cu^{++}	50	28.409	0.003	0.968	0.121	1.524	0.388	0.925	0.113
	100	66.225	0.002	0.982	0.191	0.995	0.549	0.952	0.282
	150	62.500	0.005	0.996	0.050	4.141	0.378	0.979	0.102
	200	69.524	0.015	0.997	0.213	16.069	0.192	0.864	0.316
	250	65.789	0.024	0.992	0.127	29.067	0.118	0.880	0.220
	300	73.529	0.044	0.987	0.391	48.029	0.058	0.890	0.728
Ni^{++}	50	27.778	0.002	0.945	0.014	0.424	0.541	0.878	0.094
	100	37.453	0.005	0.943	0.126	3.449	0.330	0.817	0.158
	150	61.728	0.003	0.925	0.322	2.699	0.428	0.803	0.413
	200	70.059	0.002	0.935	0.209	1.265	0.646	0.907	0.221
		Temkin isotherm constants				D–R isotherm constants			
		K_T	B	R^2	X^2	q_s	E	R^2	X^2
Cu^{++}	50	0.027	6.579	0.927	0.144	27.203	8.452	0.800	34.833
	100	0.014	15.655	0.920	0.427	36.292	8.575	0.828	123.198
	150	0.040	14.500	0.985	0.062	47.064	12.127	0.842	83.623
	200	0.700	9.002	0.886	0.285	53.710	20.412	0.836	31.104
	250	18.648	6.622	0.861	0.244	58.850	40.825	0.825	10.619
	300	174.7	5.862	0.868	0.759	66.540	158.114	0.872	3.902
Ni^{++}	50	0.013	6.528	0.860	0.1207	15.058	7.857	0.749	25.455
	100	0.054	8.127	0.814	0.1665	28.697	12.127	0.732	17.712
	150	0.030	14.252	0.786	0.4937	39.017	12.910	0.836	36.391
	200	0.018	29.629	0.948	0.3651	62.408	12.700	0.861	206.5

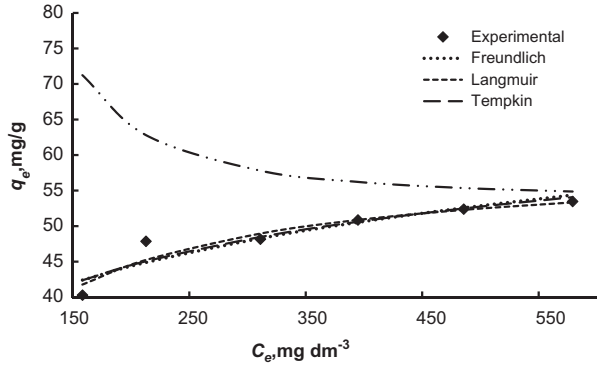

Fig. 3(a). Modeling of Cu(II) sorption onto purolite C100-MB at different initial Cu(II) concentrations (rpm = 200, temp. = 20°C, pH = 5.5, S/L = 6 g dm^{-3}).

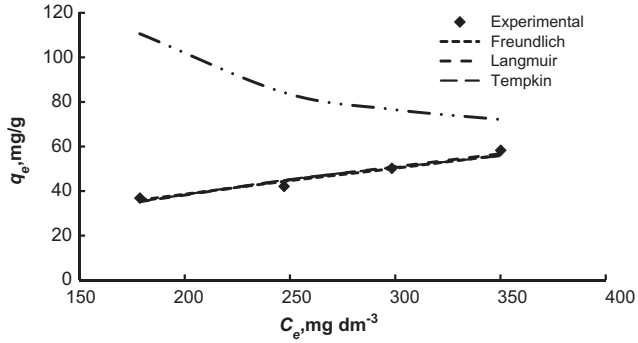

Fig. 3(b). Modeling of Ni(II) sorption onto purolite C100-MB at different initial Ni(II) concentrations (rpm = 200, temp. = 20°C, pH = 5.5, S/L = 6 g dm^{-3}).

tion by purolite C100-MB ion exchange, indicating the homogeneous surface of the ion exchange and the monolayer coverage of Cu(II) and Ni(II) ions.

3.3. Kinetic studies

3.3.1. Kinetic reaction models

The kinetics of adsorption describe the rate of metal ions uptake on ion exchange resins, which controls the equilibrium time. The kinetic of adsorbate uptake is required for selecting optimum operating conditions for the full-scale process. The kinetic parameters, which are helpful for the prediction of adsorption rate, give important information for designing and modeling the process. Adsorption kinetics were studied by applying pseudo-first order, pseudo-second order, and the Elovich equations. The pseudo-first-order model, proposed by Lagergren, assumes that the overall adsorption rate is proportional to the driving force, i.e. the difference between the average solid phase concentration and the equilibrium concentration [17]:

$$q_t = q_e(1 - e^{-k_1 t}) \tag{11}$$

Similarly, the pseudo-second-order equation, proposed by Ho [18], has been extensively applied to describe the experimental data for the sorption of organic and inorganic substances [18,19]. The equation assumes that the overall adsorption rate is proportional to the square of the driving force and can be expressed as:

$$q_t = \frac{k_2 t q_e^2}{1 + k_2 t q_e} \tag{12}$$

The Elovich model has been widely used to describe different sorption processes, which describe the adsorption process as a group of reaction mechanisms, including diffusion in the mass of dissolution, surface diffusion, and activated catalytic surfaces in the following form [20,21]:

$$q_t = \left(\frac{1}{\beta}\right) \ln(\alpha\beta) + \left(\frac{1}{\beta}\right) \ln(t) \tag{13}$$

In the previous equations, q_t (mg g^{-1}) and q_e (mg g^{-1}) are the amounts of metal adsorbed at time t and equilibrium, respectively; k_1 (min^{-1}) and k_2 (g mg^{-1} min^{-1}) are the rate constants for the pseudo-first- and pseudo-second order equations. α and β are the desorption constant and the initial adsorption rate; where α, β, $t \geq 1$.

The experimental data have been fitted by the abovementioned kinetic models for different heavy metal concentrations at 200 rpm and the obtained parameters are all listed in Table 3. Based on the analysis of the R^2 of the linear form for various kinetic models, as shown in Table 3, the pseudo-second-order model was more appropriate to describe the adsorption kinetic behavior for Cu(II) and Ni(II) ions onto the purolite C100-MB. Furthermore, the fitting results of all the three kinetic models are shown in Fig. 4. The theoretical simulated lines of the second-order model fitted the experimental data quite well, indicating a pseudo-second-order kinetic process of the adsorption of Cu(II) and Ni(II) ions onto the purolite C100-MB, and the chemisorptions were the rate-controlling mechanism. Besides, the correlation coefficients of Elovich model were also higher than 0.9 as shown in Table 3, indicating that the adsorption mechanism based on these models may be partially involved in

Table 3
Kinetic parameters for Cu (II) and Ni (II) sorption onto ion exchange resin purolite C100-MB, rpm = 200, temp. = 20°C, pH = 5.5, S/L = 6 g dm^{-3}

		Pesudo first order		Pesudo second order		Elovich equation			Intraparticle diffusion		External mass transfer	
Metal	C_0, mg L^{-1}	k_1, min^{-1}	R^2	k_2, g mg^{-1} min^{-1} × 10^4	R^2	α	β	R^2	k_{id}	R^2	k_f, cm min^{-1} × 10^3	R^2
Cu^{++}	400	0.0417	0.894	2.736	0.939	3.3061	0.0766	0.913	5.8636	0.9818	2.541	0.977
	500	0.0304	0.901	4.718	0.962	4.5616	0.0743	0.903	5.9778	0.9613	1.949	0.944
	600	0.0509	0.889	6.725	0.984	6.2503	0.0745	0.932	6.0108	0.9868	1.527	0.992
	700	0.0470	0.891	6.897	0.986	7.0312	0.0688	0.978	6.3038	0.9815	1.251	0.955
	800	0.0620	0.863	7.665	0.998	7.8950	0.0675	0.920	6.5648	0.9653	1.112	0.957
	900	0.0573	0.912	12.008	0.997	12.6166	0.0785	0.967	5.5817	0.9906	1.009	0.945
Ni^{++}	400	0.0389	0.967	3.261	0.931	3.0886	0.0836	0.940	5.3113	0.9882	4.908	0.946
	500	0.0544	0.914	1.588	0.911	3.4070	0.0659	0.937	6.7474	0.989	4.788	0.944
	600	0.0525	0.899	0.253	0.901	3.7161	0.0537	0.920	8.332	0.9841	4.648	0.928
	700	0.0419	0.925	0.255	0.912	3.9495	0.0486	0.914	9.245	0.9834	3.820	0.915

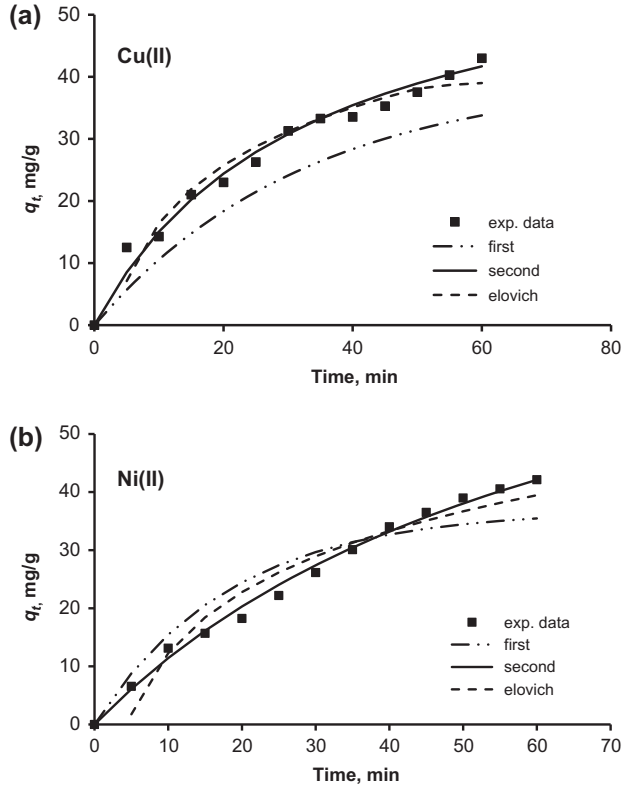

Fig. 4. Fitted curves for pseudo-first order, pseudo-second order and elovich models for adsorption kinetic data of (a) copper ions; (b) nickel ions (rpm = 200, conc. of metal ion = 500 mg dm^{-3}, pH = 5.5, S/L = 6 g dm^{-3}).

the adsorption process together with that of the pseudo-second-order kinetics.

3.3.2. Kinetic diffusion models

For a solid–liquid sorption process, the solute transfer is usually characterized by either external mass transfer (boundary layer diffusion) or intraparticle diffusion or both. The following three steps can describe the adsorption dynamics [22].

(1) The movement of adsorbate molecules from the bulk solution to the external surface of the adsorbent (film diffusion).
(2) Adsorbate molecules move to the interior part of the adsorbent particles (particle diffusion).
(3) Sorption of the solute on the interior surface of the pores and capillary spaces of adsorbent (sorption).

The ion kinetic data were processed to explore the possibility of intraparticle diffusion using the Weber–Morris equation [23]:

$$q_t = k_{id}\, t^{1/2} + c \tag{14}$$

where k_{id} is the rate constant of intraparticle diffusion and c is the film thickness. If the experimental data fit the linear behavior of Eq. (14), it can be concluded that the adsorption process is controlled by intraparticle diffusion only. If the deviation exists, it suggests that two or more steps influence the whole adsorption process. As seen in Fig. 5((a) and (b)), the plots of q_t vs. $t^{1/2}$ for Cu (II) and Ni (II) are linear over the whole time range. The plots do not go through the origin as indicative of external film control and the film mass

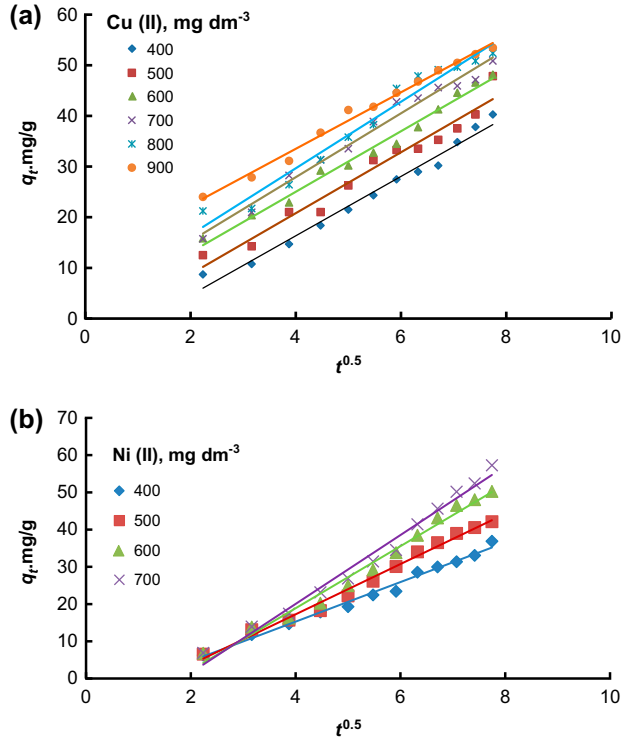

Fig. 5. Intraparticle diffusion kinetic model at different initial concentrations of (a) Cu(II) and (b) Ni(II) onto purolite C100-MB (rpm = 200,temp. = 20℃, pH = 5.5, S/L = 6 g dm^{-3}).

transfer parameters can be determined from the kinetic equation presented by McKay and Allen; [24]. The equation is often applied to model the external diffusion, during the migration of aqueous adsorbates from a liquid phase to the solid adsorbent :

$$\ln\left(\frac{C_t}{C_0}-\frac{1}{1+m_sK}\right)=\ln\left(\frac{m_sK}{1+m_sK}\right)-\frac{1+m_sK}{m_sK}k_fS_st \tag{15}$$

where m_s (g dm^{-3}) is the mass of resin per unit volume of particle-free slurry, K (Q_mK_L) ($dm^3\,g^{-1}$) is the Langmuir constants, S_s (cm^{-1}) is specific particle surface area for mass transfer, d_p (cm) is particle diameter, ρ_p (g dm^{-3}) is the density of resin particles, and ε_p is the porosity of resin particles. The surface area for external mass transfer to the particles can be obtained from m_s which is defined as the concentration of the adsorbent in the liquid phase:

$$m_s=\frac{M}{V} \tag{16}$$

The specific surface, S_s, of a particle for external mass transfer is:

$$S_s=\frac{6m_s}{d_p\rho_p(1-\varepsilon_p)} \tag{17}$$

The external mass transfer coefficient, k_f, can be obtained from equation (15) by plotting $\ln\left(\frac{C_t}{C_0}-\frac{1}{1+m_sK}\right)$ vs. time. The parameters calculated from the data fitting are summarized in Table 3.

According to the external diffusion equation (Eq. (15)) and the intraparticle diffusion model, it was found that the initial heavy metal concentration influences the process kinetics. The intraparticle diffusion constants generally increase with increasing the concentration for the two heavy metals while, external mass transfer diffusion coefficient decreases with the increase in concentration of heavy metals.

It appears that the kinetics of heavy metals adsorption is controlled by external diffusion mechanism during the first stages specially at low concentrations since the intraparticle resistance is negligible, and the transport of the aqueous species towards the solid phase is mainly ensured by the external diffusion mechanism [25]. While, the rate was dominated by the diffusion of heavy metals through the solid/liquid interface during the entire process of ion exchange.

3.4. Thermodynamics studies

To further understand the energetic of the adsorption processes, thermodynamic parameters: enthalpy change (ΔH°, kJ mol^{-1}) and entropy change (ΔS°, J $mol^{-1}\,K^{-1}$) were calculated using Van't Hoff equation from the slope and intercept of a plot of ln K_d against $1/T$ via the following equation [26]:

$$\ln K_d=\frac{\Delta S^\circ}{R}-\frac{\Delta H^\circ}{RT} \tag{18}$$

The distribution coefficient, K_d, was calculated using the following equation:

$$K_d=\frac{q_e}{C_e} \tag{19}$$

where T is the temperature (K), R is the gas constant (J $mol^{-1}\,K^{-1}$), ΔH° is the molar enthalpy change (J mol^{-1}), and, ΔS° is the molar entropy change (J $mol^{-1}\,K^{-1}$).

The free energy change of the adsorption reaction (ΔG°) can be calculated using the following equation:

$$\Delta G^{\circ} = \Delta H^{\circ} - T\Delta S^{\circ} \quad (20)$$

The positive value of ΔH° for Cu(II) and Ni(II) shows that the sorption process is endothermic (Table 4). The endothermicity of the ion exchange process may be due to the removal of water molecules from the solid/solution interface and from the sorbing cation. The ΔG° is negative and decreases with increasing temperature, implying that the reaction is spontaneous and favored by higher temperature. The entropy changes in this study are found to be positive; it means that the increased randomness appeared on the resin–solution interface during the exchange of heavy metal [27]. Table 4 shows the thermodynamic parameters of copper and nickel which are in agreement with previous studies [28–30].

3.5. Adsorption selectivity of metal ions at different metal ratio

The distribution of each of the metal ions between the resin phase and the aqueous phase was determined at room temperature at various Cu(II) to Ni(II) ratios, batch experiments were carried out at optimal conditions of pH = 5.5; resin dosage ratio = 6 g dm^{-3} using 400 mg dm^{-3} metal ion concentration, the results are presented in Fig. 6. The effect of Cu(II) to Ni(II) ratio on the amount of metal ions distributed between the two phases are given in Table 5, indicating that Cu(II) and Ni(II) ions have highest distribution ratio using the 1:1 Cu(II) to Ni(II) ratio. The results also indicate that the purolite C100-MB resin takes up Cu (II) ions more selectively than Ni(II) ions at pH 5.5.

3.6. Desorption study

One of the major advantages of ion exchange resin is that it could be regenerated and reused. The regenerated resin was reused up to four adsorption–desorption cycles and the results are illustrated in Fig. 7. It was clear that the adsorption capacity for Cu (II) and Ni (II) decreases slightly after many cycles. This might be due to the amount of ion exchange lost during the adsorption–desorption cycles. The decrease in the capacity of adsorption was about 50% of its initial value, which showed that the adsorbent had a good potential to adsorb copper and nickel ions, even though it has been reused for few times.

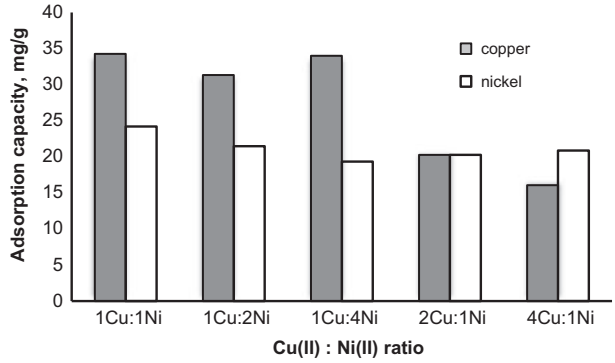

Fig. 6. Adsorption selectivity of metal ions at different metal ratio.

Table 5
Distribution coefficient of different metal ion uptake at different metal ratios

	Distribution coefficient (K_D) of various metal ion uptake	
Cu(II) : Ni(II)	Cu(II)	Ni(II)
1:1	174.16	94.57
1:2	146.29	79.15
1:4	170.20	70.08
2:1	84.29	83.66
4:1	54.23	74.18

Table 4
Thermodynamic parameters for Cu (II) and Ni (II) on purolite C100-MB

M^{++}	rpm	ΔH°	ΔS°	ΔG°_{293}	ΔG°_{303}	ΔG°_{313}	ΔG°_{323}	R^2
Cu^{++}	50	17,727	34.51	−27,841	−28,186	−28,532	−28,877	0.960
	100	13,187	22.85	−19,885	−2011	−20,342	−20,570	0.982
	150	9,404	14.19	−13,563	−13,705	−13,847	−13,989	0.923
	200	2,279	4.58	−3,624	−3,670	−3,716	−3,762	0.996
Ni^{++}	50	23,279	49.89	−37,896	−38,395	−38,894	−39,393	0.808
	100	18,510	43.31	−31,201	−31,635	−32,068	−32,501	0.948
	150	15,314	37.71	−26,365	−26,742	−27,119	−27,497	0.975
	200	13,576	23.15	−20,360	−20,592	−20,824	−21,055	0.949

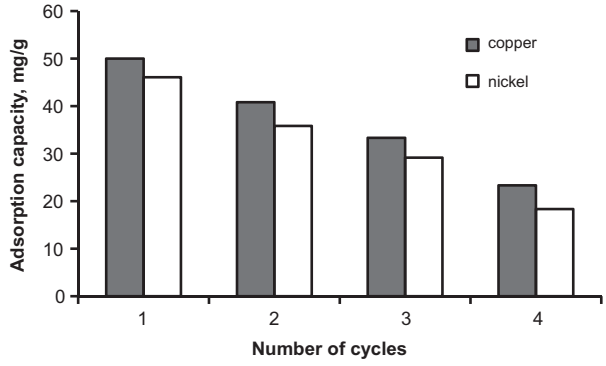

Fig. 7. The performance of purolite C100-MB after multiple cycles of regeneration.

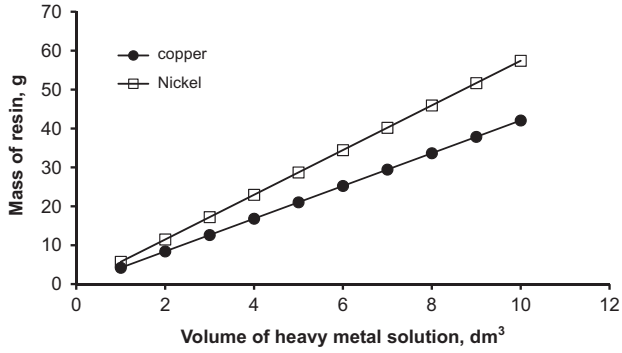

Fig. 8. Mass of resin (M) against volume of heavy metal solution treated (dm^3).

3.7. Designing batch adsorption from equilibrium data

An empirical design procedure based on sorption equilibrium conditions is the most common method for predicting the size of ion exchange column and performance. Adsorption isotherms can be used to predict the design of single-stage batch ion exchange system [31]. The design objective is to reduce the copper(II) or nickel(II) ion concentration from C_0 (mg dm^{-3}) to C_f (mg dm^{-3}) of solution volume V (dm^3). The amount of ion exchange is M (g) and the heavy metal ion loading changes from q_0 (mg g^{-1}) to q_f (mg g^{-1}). At time $t = 0$, $q_0 = 0$ as time proceeds and the mass balance equates the Cu (II) or Ni(II) ion removed from the aqueous solution to that picked by the resin. The mass balance for the single-stage batch adsorption system can be given as:

$$V(C_0 - C_f) = M(q_0 - q_f) = Mq_f \tag{21}$$

At equilibrium conditions $C_f \rightarrow C_e$ and $q_f \rightarrow q_e$.

Since adsorption isotherm studies fits well in Langumuir adsorption isotherm, it is used for q_f in equation batch adsorption design. Rearranging Eq. (21), we get:

$$\frac{M}{V} = \frac{(C_0 - C_f)}{q_f} = \frac{C_0 - C_e}{q_e} = \frac{C_0 - C_e}{\frac{Q_m K_L C_e}{1 + K_L C_e}} \tag{22}$$

Fig. 8 shows the plot between the calculated amounts of resin required to remove Cu(II) or Ni(II) ions from solution of initial concentration 400 mg dm^{-3} for 60 and 55% for Cu(II) and Ni(II), respectively, at different solution volumes (1–10 dm^3) for a single-stage batch ion exchange system, for which the design procedure is outlined. For example, the amount of purolite C100-MB resin required for the 60% removal of Cu(II) ion solution of concentration 400 mg dm^{-3} was 4.2 g for each liter of copper ion solution. While 5.74 g of the same resin is required for 55% removal of Ni(II) ions from an aqueous solution of 400 mg dm^{-3} concentration.

4. Conclusions

The removal of copper and nickel ions from aqueous solutions by cation exchange resin, purolite C100-MB, packed in a perforated basket rotating reactor were studied. The optimum adsorption pH was about 5.5. Equilibrium data have been analyzed using Langmuir, Freundlich, Tempkin, and Dubinin Radushkevich isotherms. Langmuir isotherm provides the best fit to the experimental data indicating homogeneous adsorption and monolayer coverage of metal ion on ion exchange. From the kinetic studies, it was found that adsorption equilibrium can be reached in 60 min and the adsorption processes followed pseudo-second-order model for Cu(II) and Ni(II). Kinetics of copper and nickel ions adsorption were controlled by external diffusion mechanism during the first stages specially at low concentrations while the rate was dominated by the diffusion of heavy metals through the solid/liquid interface during the entire process of adsorption. Thermodynamic parameters were calculated. The sorption process of metal ions into purlite C100-MB was spontaneous and endothermic process. The present study indicated that the purolite C100-MB resin packed in rotating basket reactor had selelectivity to Cu(II) ions more than Ni(II) ions at pH 5.5. An empirical batch design equation based on sorption equilibrium (Langmuir isotherm) was estimated. Furthermore, the resin had a good potential material to adsorb metal ions though it has been reused for few times.

References

[1] Z. Jin, D.-X. Xie, X.-B. Zhang, Y.-J. Gong, W. Tan, Bifunctional fluoroionphore-ionic liquid hybrid for toxic heavy metal ions: Improving its performance via the synergistic extraction strategy, Analyt. Chem. 84 (2012) 4253–4257.

[2] S.A. El-Safty, M.A. Shenashen, A.A. Ismail, A multi-pH-dependent, single optical mesosensor/captor design for toxic metals, Chem. Commun. 48 (2012) 9652–9654.

[3] M.A. Shenashen, S.A. El-Safty, E.A. Elshehy, Architecture of optical sensor for recognition of multiple toxic metal ions from water, J. Hazard. Mater. 260 (2013) 833–843.

[4] EPA, U.S. Edition of the Drinking Water Standards and Health Advisories, U.S. Environmental Protection Agency, Washington, DC, 2012 (EPA 822-S-April).

[5] K.A. Krishnan, K.G. Sreejalekshmi, R.S. Baiju, Nickel (II) adsorption onto biomass based activated carbon obtained from sugarcane bagasse pith, Bioresour. Technol. 102 (2012) 10239–10247.

[6] D.W. O'Connell, C. Birkinshaw, T.F. O'Dwyer, Heavy metal adsorbents prepared from the modification of cellulose: A review, Bioresour. Technol. 99 (2008) 6709–6724.

[7] Q. Yuan, N. Li, Y. Chi, W. Geng, W. Yan, Y. Zhao, X. Li, B. Dong, Effect of large pore size of multifunctional mesoporous microsphere on removal of heavy metal ions, J. Hazard. Mater. 254–255 (2013) 157–165.

[8] B. Li, F. Liu, J. Wang, C. Ling, L. Li, P. Hou, A. Li, Z. Bai, Efficient separation and high selectivity for nickel from cobalt-solution by a novel chelating resin: Batch, column and competition investigation, Chem. Eng. J. 195–196 (2012) 31–39.

[9] S. Malamis, E. Katsou, A review on zinc and nickel adsorption on natural and modified zeolite, bentonite and vermiculite: Examination of process parameters, kinetics and isotherms, J. Hazard. Mater. 252-253 (2013) 428–461.

[10] M.A. Ahamed, D. Jeyakumar, A.R. Burkanudeen, Removal of cations using ion-binding terpolymer involving 2-amino-6-nitro-benzothiazole and thiosemicarbazide with formaldehyde by batch equilibrium technique, J. Hazard. Mater. 248–249 (2013) 59–68.

[11] M.A. Hossain, H.H. Ngo, W.S. Guo, T. Setiadi, Adsorption and desorption of copper(II) ions onto garden grass, Bioresour. Technol. 121 (2012) 386–395.

[12] J.J. Chen, A.L. Ahmad, B.S. Ooi, Poly(N-isopropylacrylamide-co-acrylic acid) hydrogels for copper ion adsorption: Equilibrium isotherms, kinetic and thermodynamic studies, J. Environ. Chem. Eng. 1 (2013) 339–348.

[13] O. Abollino, M. Aceto, M. Malandrino, C. Sarzanini, E. Mentasti, Adsorption of heavy metals on Na-montmorillonite. Effect of pH and organic substances, Water Res. 37 (2003) 1619–1627.

[14] O. Abollino, A. Giacomino, M. Malandrino, E. Mentasti, Interaction of metal ions with montmorillonite and vermiculite, Appl. Clay Sci. 38 (2008) 227–236.

[15] A.E. Nemr, A. El-Sikaily, A. Khaled, O. Abdelwahab, Removal of toxic chromium from aqueous solution, wastewater and saline water by marine red alga *Pterocladia capillacea* and its activated carbon, Arab. J. Chem. (2011). doi:10.1016/j.arabjc.2011.01.016.

[16] O. Abdelwahab, N.K. Amin, E-S.Z El-Ashtoukhy, Removal of zinc ions from aqueous solution using a cation exchange resin, Chem. Eng. Res. Des. 91 (2013) 165–173.

[17] C.S. Sundaram, N. Viswanathan, S. Meenakshi, Defluoridation chemistry of synthetic hydroxyapatite at nano scale: equilibrium and kinetic studies, J. Hazard. Mater. 155 (2008) 206–215.

[18] Y.S. Ho, Review of second-order models for adsorption systems, J. Hazard. Mater. 136 (2006) 681–689.

[19] Y.S. Ho, G. McKay, The kinetics of sorption of divalent metal ions onto *Sphagnum moss* peat, Water Res. 34 (2000) 735–742.

[20] C. Valderrama, J. Cortina, A. Farran, X. Gamisans, C. Lao, Kinetics of sorption of polyaromatic hydrocarbons onto granular activated carbon and Macronet hyper-cross-linked polymers (MN200), J. Colloid Interface Sci. 310 (2007) 35–46.

[21] C. Valderrama, J.I. Barios, M. Caetano, A. Farran, J.L. Cortina, Kinetic evaluation of phenol/aniline mixtures adsorption from aqueous solutions onto activated carbon and hypercrosslinked polymeric resin (MN200), React. Funct. Polym. 70 (2010) 142–150.

[22] P.S. Kumar, S. Ramalingam, S. Dinesh Kirupha, A. Murugesan, T. Vidhyadevi, S. Sivanesan, Adsorption behavior of nickel(II) onto cashew nut shell: Equilibrium, thermodynamics, kinetics, mechanism and process design, Chem. Eng. J. 167 (2011) 122–131.

[23] W. Weber, J. Morris, Kinetics of adsorption on carbon from solution, J. Sanit. Eng. Div. Am. Soc. Civ. Eng. 89 (1963) 31–60.

[24] G. McKay, S.J. Allen, Surface mass transfer processes using peat as an adsorbent for dyestuffs, Can. J. Chem. Eng. 58 (1980) 521–526.

[25] T. Ozlem, H. Tanaci, Z. Aksu, Potential use of cotton plant wastes for the removal of Remazol Black B reactive dye, J. Hazard. Mater. 163 (2009) 187–198.

[26] A.R. Kul, H. Koyuncu, Adsorption of Pb(II) ions from aqueous solution by native and activated bentonite: Kinetic, equilibrium and thermodynamic study, J. Hazard. Mater. 179 (2010) 332–339.

[27] H. Lee, Y.-C. Kuan, J.-M. Chern, Equilibrium and kinetics of heavy metal ion exchange, J. Chin. Inst. Chem. Eng. 38 (2007) 71–84.

[28] S. Svilović, D. Rušić, R. Zanetić, Thermodynamics and adsorption isotherms of copper ions removal from solutions using synthetic zeolite X, Chem. Biochem. Eng. Q. 22(3) (2008) 299–305.

[29] P.U. Singare, R.S. Lokhande, R. D'Souza, Thermodynamics of uni-univalent ion exchange reactions using strongly acidic cation exchange resin TULSION T-46, Rasayan J. Chem. 2(3) (2009) 645–648.

[30] J. Kabuba, F. Ntuli, E. Muzenda, M. Mollagee, Thermodynamics of Cu (II) adsorption onto South African clinoptilolite from synthetic solution by ion exchange process, 2nd International Conference on Chemistry and Chemical Engineering, IPCBEE, Chengdu, Vol. 14, 2011.

[31] V. Vadivelan, K.V. Kumar, Equilibrium, kinetics, mechanism, and process design for the sorption of methylene blue onto rice husk, J. Colloid Interface Sci. 286 (2005) 90–100.